# The antihelmenthic phosphate niclosamide impedes renal fibrosis by inhibiting homeodomain-interacting protein kinase 2 expression

Xiaoyan Chang[1,3], Xin Zhen[1,3], Jixing Liu[1], Xiaomei Ren[2], Zheng Hu[1], Zhanmei Zhou[1], Fengxin Zhu[1], Ke Ding[2] and Jing Nie[1,3]

[1]State Key Laboratory of Organ Failure Research, National Clinical Research Center of Kidney Disease, Key Laboratory of Organ Failure Research, Ministry of Education, and Division of Nephrology, Nanfang Hospital, Southern Medical University, Guangzhou, China; and [2]School of Pharmacy, Jinan University, Guangzhou, China

**Renal fibrosis is the final common pathway of all varieties of progressive chronic kidney disease. However, there are no effective therapies to prevent or slow the progression of renal fibrosis. Niclosamide is a US Food and Drug Administration–approved oral antihelminthic drug used for treating most tapeworm infections. Here, we demonstrated that phosphate niclosamide, the water-soluble form of niclosamide, significantly reduced proteinuria, glomerulosclrotic lesions, and interstitial fibrosis in a murine model of adriamycin nephropathy. In addition, phosphate niclosamide significantly ameliorated established renal interstitial fibrosis a murine model of unilateral ureteral obstruction. Mechanistically, phosphate niclosamide directly inhibited TGF-β-induced expression of homeodomain-interacting protein kinase 2 (HIPK2) by interfering with the binding of Smad3 to the promoter of the HIPK2 gene, and subsequently mitigated the activation of its downstream signaling pathways including Smad, Notch, NF-κB and Wnt/β-catenin pathway both *in vitro* and *in vivo*. Thus, phosphate niclosamide mitigates renal fibrosis at least partially by inhibiting HIPK2 expression. Hence, phosphate niclosamide might be a potential therapeutic agent for renal fibrosis.**

*Kidney International* (2017) **92,** 612–624; http://dx.doi.org/10.1016/j.kint.2017.01.018

KEYWORDS: HIPK2; Notch; phosphate niclosamide; renal fibrosis; Smad; Wnt/β-catenin



**Correspondence:** *Jing Nie, Division of Nephrology, Nanfang Hospital, Southern Medical University, North Guangzhou Avenue 1838, Guangzhou 510515, People's Republic of China. E-mail: niejing@smu.edu.cn*

[3]These authors contribute equally to this work.

**Received 19 September 2016; revised 15 January 2017; accepted 19 January 2017; published online 17 March 2017**

The prevalence of chronic kidney disease in the general population is high and is increasing worldwide.[1,2] Renal fibrosis is the final common pathway of all kinds of progressive chronic kidney disease leading to end-stage renal disease.[3–6] Although great efforts have been made in recent years, there are no effective therapies to prevent or slow the progression of renal fibrosis,[5] and the treatment options for patients with end-stage renal disease are limited to dialysis and renal transplantation. Therefore, it is imperative to develop satisfactory therapeutic drugs for renal fibrosis.

One promising approach to slow the progression of fibrosis is to target important fibrogenic pathways. Accumulating studies have shown that multiple signaling pathways such as transforming growth factor (TGF)-β/Smads, Wnt/β-catenin, mTOR (mechanistic target of rapamycin), nuclear factor κB (NF- κB), and Notch are critical in the pathogenesis of renal fibrosis.[3,5,7] Recently, homeodomain-interacting protein kinase 2 (HIPK2), a member of an evolutionary conserved family of serine/threonine kinases, has been identified as a key regulator in kidney fibrosis and idiopathic pulmonary fibrosis that acts upstream of several major profibrotic and proinflammatory pathways including TGF-β/Smad, Wnt/β-catenin, Notch pathway, and NF-κB pathway,[8–11] indicating that HIPK2 might be a potential target for antifibrosis therapy.[5,9,12]

Niclosamide (NICLO), whose systematic name is (5-chloro-N-2-chloro-4-nitrophenyl)-2-hydroxybenzamide, is a US Food and Drug Administration–approved oral antihelminthic drug used for treating most tapeworm infections.[13] It is also used as a molluscicide for water treatment in schistosomiasis control programs.[13,14] The activity of NICLO against these parasites is believed to be mediated by inhibiting mitochondrial oxidative phosphorylation and anaerobic adenosine triphosphate production.[13,15] High-throughput screening campaigns have identified NICLO as a potential anticancer agent.[14,16–18] However, NICLO has poor water solubility.[13,19] To improve its water solubility, a phosphate of NICLO (P-NICLO) is synthesized and has been proven to be able to induce apoptosis of acute myelogenous leukemia cells.[13,20]

It has been shown that P-NICLO exerts antitumor function by targeting multiple signaling pathways including NF-κB, Wnt/β-catenin, and the Notch pathway.[13,14] Given the critical role of these pathways in the pathogenesis of renal fibrosis, the aim of this study was to explore the potential therapeutic effect of P-NICLO on renal fibrosis. We found that administration of P-NICLO significantly inhibited the progression of renal fibrosis in adriamycin (ADR) nephropathy and unilateral ureteral obstruction (UUO) models. Mechanistically, the antifibrotic effect of P-NICLO was at least partially mediated by inhibiting TGF-β1–induced HIPK2 expression and the activation of its downstream multiple profibrotic pathways.

## RESULTS

### P-NICLO attenuates glomerular injury and interstitial fibrosis induced by ADR

We first investigated the effects of P-NICLO on ADR nephropathy, a model characterized by initial podocyte injury and albuminuria and subsequent renal fibrosis. BALB/c mice were injected with ADR, and 2 weeks later, mice were given P-NICLO (30 mg/kg per day) by i.p. injection. As shown in Figure 1a, at 5 weeks after ADR injection, albuminuria was markedly elevated in the ADR group compared with the control group, P-NICLO administration significantly attenuated ADR-induced albuminuria. In addition, periodic acid–Schiff staining showed attenuated glomerulosclerosis, as evidenced by decreased mesangial expansion and less accumulation of extracellular matrix in the mesangium of P-NICLO–treated mice (Figure 1b). A semiquantitative glomerulosclerotic index of kidney sections confirmed that P-NICLO administration led to a marked reduction in the index (Figure 1c), suggesting that P-NICLO attenuates ADR nephropathy.

We further examined the effects of P-NICLO on interstitial fibrosis. As shown in Figure 1d–f, Western blot and immunohistochemistry staining revealed marked upregulation of α-smooth muscle actin (α-SMA), fibronectin, and collagen I at 5 weeks after ADR injection. Administration of P-NICLO significantly attenuated their induction together with reduced interstitial collagen deposition (Figure 1g and h). These data indicate that P-NICLO attenuates ADR-induced interstitial fibrosis.

### P-NICLO inhibits multiple profibrotic signaling pathways *in vitro* and *in vivo*

Previous studies show that niclosamide could inhibit the activity of Wnt/β-catenin and Notch signaling, which are implicated in renal fibrosis.[13,21–24] Therefore, we evaluated whether P-NICLO could affect their activity. NRK52E cells were incubated with 10 ng/ml of TGF-β1 with or without P-NICLO for 24 hours, and cell lysate was harvested. As shown in Figure 2c and d, P-NICLO significantly inhibited TGF-β1–induced expression of *PAI-1*, *MMP-7*, and *Snail*, which are the target genes of Wnt/β-catenin, and expression of *Hes1*, *Hey1*, and *Hey2*, which are the target genes of Notch signaling. In addition, P-NICLO attenuated TGF-β1–induced Smad3 phosphorylation in a dose-dependent manner (Figure 2a and b). Consistently, the levels of p-Smad3, PAI-1, MMP-7, Snail, Hes1, Hey1, and Hey2 in the ADR model were significantly inhibited by p-NICLO (Figure 3). Collectively, these data suggest that P-NICLO inhibits the activation of multiple profibrotic pathways.

### P-NICLO inhibits the expression of profibrosis markers through targeting HIPK2

Because HIPK2, a key regulator in kidney fibrosis, acts upstream of multiple antifibrotic pathways,[8–10,12] we hypothesized that HIPK2 might be the target of P-NICLO. To test this hypothesis *in vitro*, we first examined the cytotoxicity of P-NICLO by MTT assay. Rat proximal tubular cells (NRK52E) were incubated with the indicated amount of P-NICLO for 24 hours and then harvested for analysis. No obvious cell mortality was observed when cells were incubated with as much as 4 μM of P-NICLO (Supplementary Figure S1). Therefore, 0 to 2 μM of P-NICLO was used for the following experiments.

First, we examined whether P-NICLO could modulate the expression of HIPK2. NRK52E cells were incubated with 10 ng/ml of TGF-β1 with or without P-NICLO for 24 hours. Consistent with a previous study,[8] TGF-β1 significantly upregulated HIPK2 expression at both mRNA and protein levels measured by Western blot and real-time polymerase chain reaction (PCR). P-NICLO significantly attenuated TGF-β1–augmented HIPK2 expression in a dose-dependent manner (Figure 4a–c). Similarly, Western blot and real-time PCR showed that the expression of renal HIPK2 in the ADR model was inhibited by P-NICLO treatment (Figure 4d–f). Bioinformatic analysis revealed a putative Smad3 binding motif on the promoter region of both human and murine *HIPK2* genes (Figure 4g). Chromatin immunoprecipitation assay demonstrated the binding of Smad3 on the promoter region of the human *HIPK2* gene in human proximal tubular (HK-2) cells. The amount of Smad3 on the promoter of HIPK2 was significantly attenuated by P-NICLO (Figure 4h). These data indicate that P-NICLO inhibits HIPK2 transcription by interfering with the binding of Smad3 to the promoter region of the *HIPK2* gene.

To further confirm that the antifibrotic effect of P-NICLO is mediated by HIPK2, HIPK2 was overexpressed in HK-2 cells by transient transfection of the expression construct WT-HIPK2. As shown in Figure 5a and b, P-NICLO treatment inhibited TGF-β–increased phosphorylation of Smad3. However, this inhibitory effect of P-NICLO was significantly diminished in cells overexpressing HIPK2. Moreover, real-time PCR showed that HIPK2 overexpression partially attenuated the inhibitory effect of P-NICLO on TGF-β1–augmented transcription of profibrotic markers such as vimentin and fibronectin (Figure 5c).

### P-NICLO attenuates NF-κB activation and renal inflammation *in vitro* and *in vivo*

NF-κB is downstream of HIPK2.[8,12] We examined the effects of P-NICLO on TGF-β1–induced NF-κB activation. NRK52E cells were incubated with 10 ng/ml of TGF-β1 with or

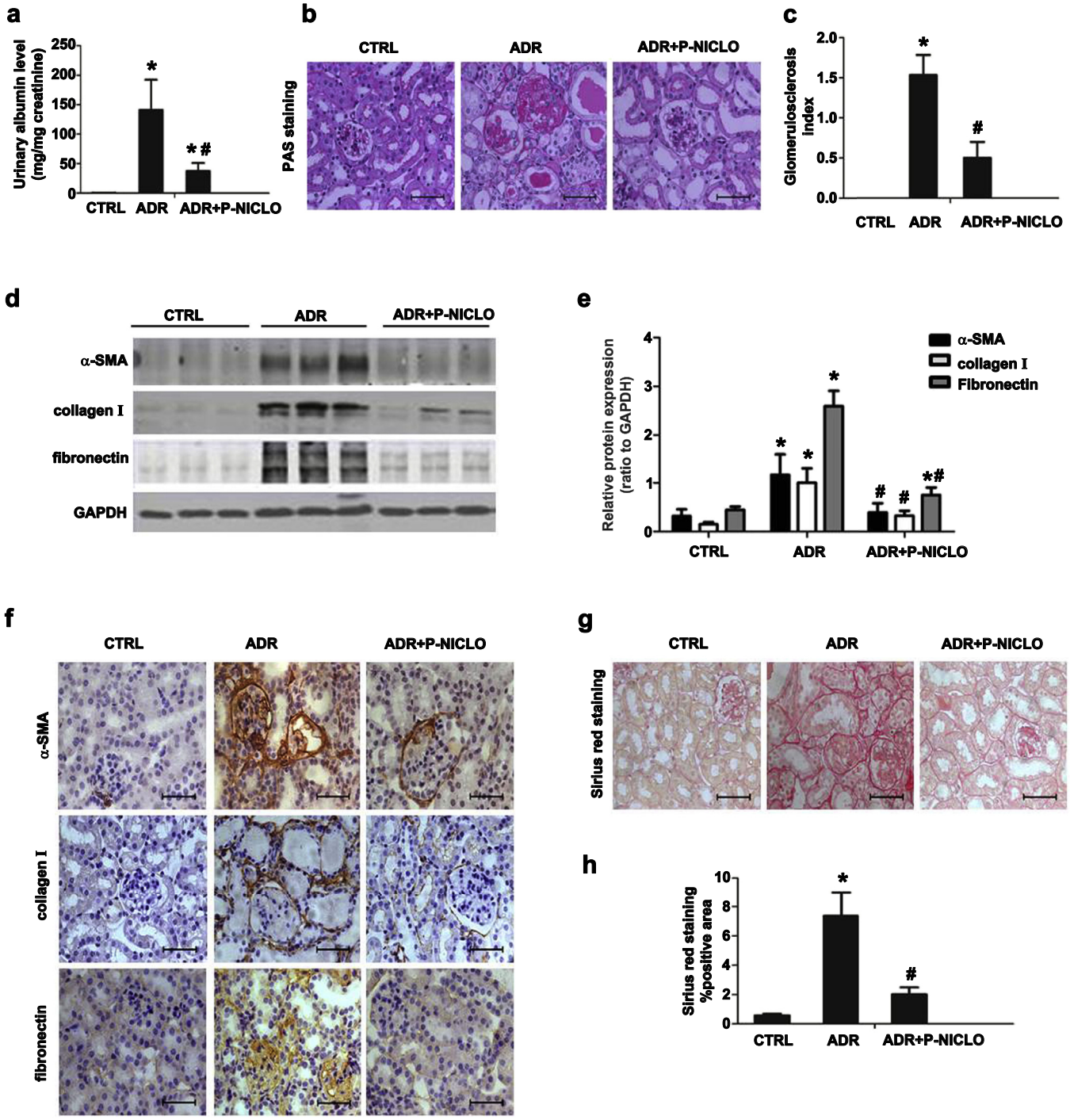


**Figure 1 | Phosphate of niclosamide (P-NICLO) ameliorates glomerular injury and interstitial fibrosis in ADR nephropathy.** (**a**) Urinary albumin levels expressed as mg/mg creatinine in different groups of mice at 5 weeks after DOX injection. (**b**) Representative micrographs show glomerular injury based on periodic acid–Schiff (PAS) staining. (**c**) Glomerulosclerosis index (GSI) in different groups of mice. (**d,e**) Western blots show the upregulation of α-smooth muscle actin (α-SMA), collagen I, and fibronectin in kidney cortex at 5 weeks after DOX injection in different groups of mice. Representative Western blots (**d**) and quantitative data (**e**) are presented. (**f**) Representative micrographs of immunohistochemical staining of α-SMA, collagen I, and fibronectin in the renal cortex are presented. Representative micrographs of Sirius red staining (**g**) and (**h**) quantitative assessment of interstitial collagen accumulation based on Sirius red staining are presented. Bar = 50 μm. Data are expressed as mean ± SD, $N = 5$. *$P < 0.05$ versus control (CTRL) group. #$P < 0.05$ versus DOX group. GAPDH, glyceraldehyde-3-phosphate dehydrogenase. To optimize viewing of this image, please see the online version of this article at www.kidney-international.org.

without P-NICLO for 24 hours, and cell lysate was harvested. Western blot revealed that the level of phosphorylated p65 (p-p65) was increased by TGF-β1, and this augmentation was substantially inhibited by P-NICLO treatment (Figure 6a and b). In addition, real-time PCR revealed that expression of *CCL2*, *CCL20*, *ICAM-1*, and *Fas*, the target genes of NF-κB,

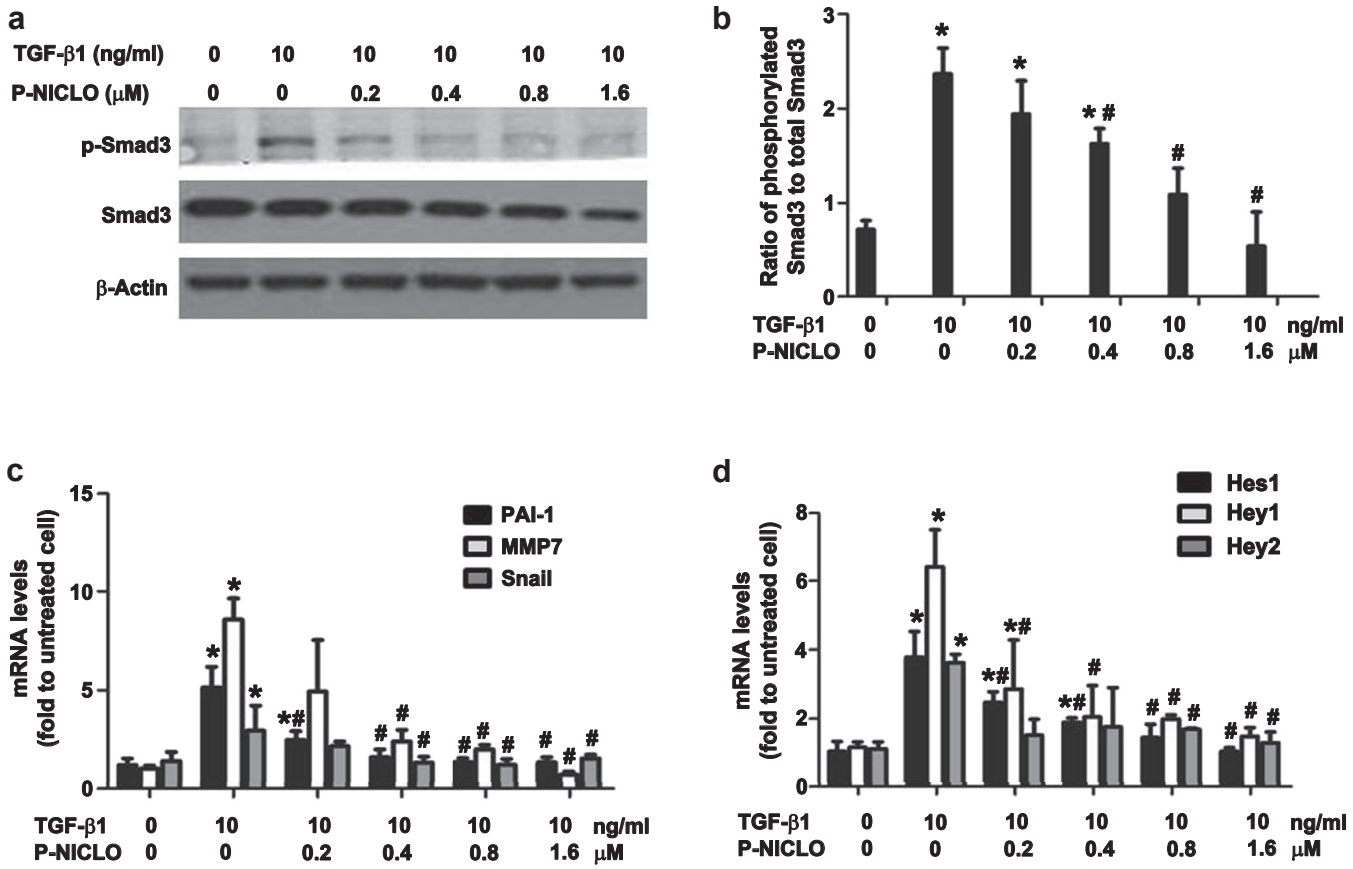


**Figure 2 | Phosphate of niclosamide (P-NICLO) inhibits multiple profibrotic signaling pathways *in vitro*.** NRK52E cells were preincubated with or without the indicated amount of P-NICLO for 1 hour and then coincubated with transforming growth factor-β1 (TGF-β1) (10 ng/ml) for 24 hours. (**a**) Western blots show the protein level of phosphorylated Smad3 (p-Smad3). (**b**) Graphic representation of the relative abundance of p-Smad3 normalized with its total protein. The expression of the target genes of Wnt/β-Catenin signaling (**c**) and the target genes of Notch signaling (**d**) were determined by real-time polymerase chain reaction and presented as fold induction over untreated cells. Data are expressed as the mean ± SD of 3 independent experiments. *$P < 0.05$ versus untreated cells. #$P < 0.05$ versus TGF-β1–treated cells. To optimize viewing of this image, please see the online version of this article at www.kidney-international.org.

was also inhibited by P-NICLO (Figure 6c and d). These data suggest that P-NICLO inhibits TGF-β1–induced NF-κB activation *in vitro*.

We next examined the effects of P-NICLO on ADR-induced renal inflammation *in vivo*. In line with *in vitro* data, Western blot and real-time PCR showed that P-NICLO substantially inhibited ADR-augmented p-p65 and the expression of its target genes (Figure 6e–h). In addition, P-NICLO inhibited renal expression of proinflammatory cytokines tumor necrosis factor-α, monocyte chemotactic protein-1, and intereleukin-6 (Supplementary Figure S2). These data suggest that P-NICLO attenuates renal inflammation by inhibiting NF-κB activation.

### P-NICLO ameliorates established renal fibrosis induced by UUO

To investigate the therapeutic effect of P-NICLO on renal fibrosis, we generated the typical mouse model of renal interstitial fibrosis induced by UUO. At day 7 after UUO, P-NICLO (30 mg/kg per day) was given by i.p. injection. Immunohistochemistry staining and Western blot analysis of whole-kidney lysates indicated that P-NICLO significantly inhibited the upregulation of α-SMA, collagen I, and fibronectin (Figure 7a–c). The reduced collagen deposition and extracellular matrix accumulation was confirmed by picrosirius red staining (Figure 7d and e) and Masson trichrome staining (Figure 7f and g). These data suggest that P-NICLO could attenuate established renal fibrosis.

Consistently, the expression of HIPK2 and the level of p-Smad3 and p-p65 were decreased in renal tissue of P-NICLO–treated mice (Figure 8a–f). In addition, real- time PCR revealed that expression of target genes of Wnt/β-catenin (Figure 8g–i) and Notch signaling (Figure 8j) were all significantly decreased in P-NICLO–treated mice.

We further assessed the effect of P-NICLO on interstitial inflammation in UUO. As shown in Supplementary Figure S3A–C, the number of $CD3^+$ T cells and $F4/80^+$ macrophages infiltrated in the tubular interstitium was significantly decreased in mice treated with P-NICLO at day 14 after UUO, suggesting that P-NICLO treatment significantly reduced inflammatory cell infiltration. Quantative real-time PCR showed that the upregulation of the target genes of NF-κB

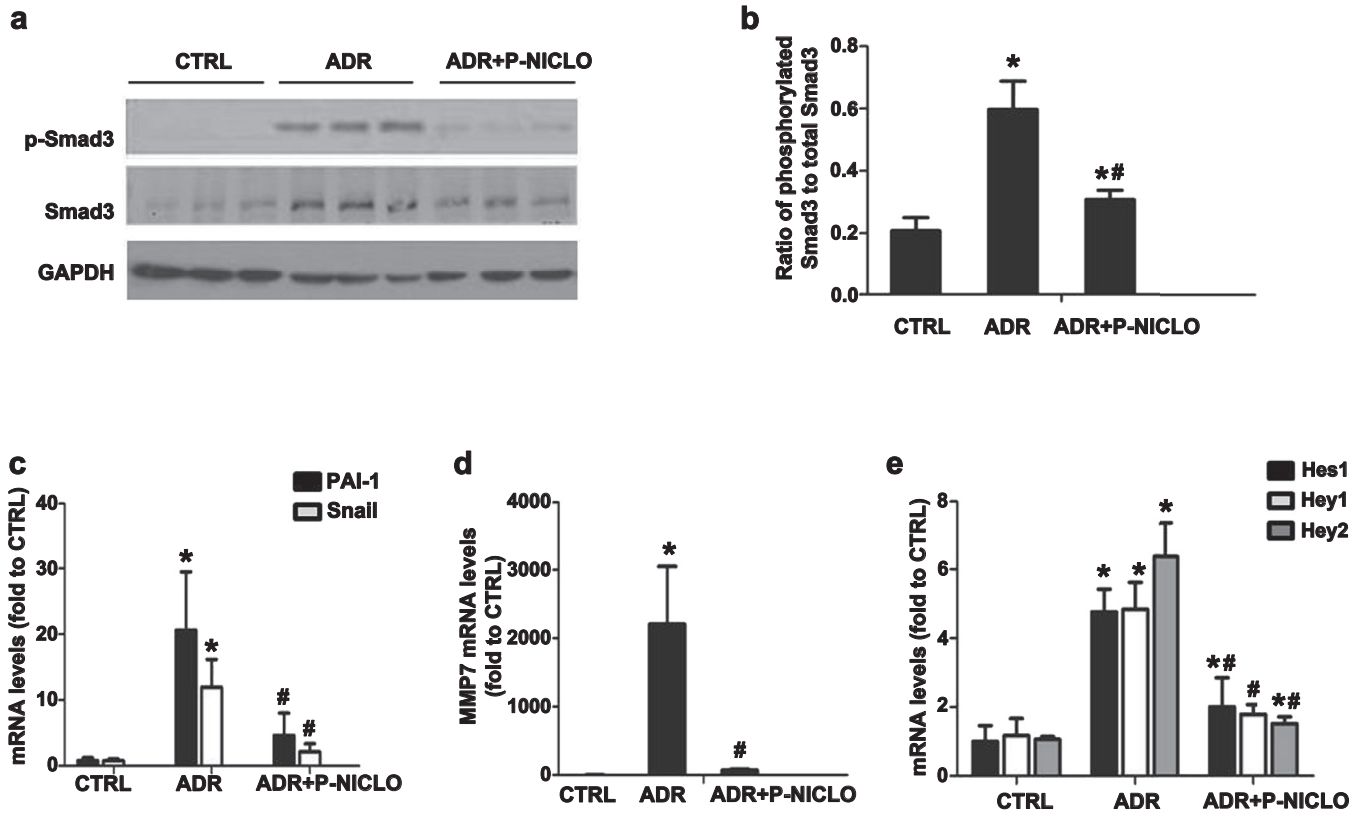


**Figure 3 | Phosphate of niclosamide (P-NICLO) inhibits multiple profibrotic signaling pathways in ADR nephropathy.** (**a**) Representative Western blots show the level of p-Smad3 in the renal cortex of different groups of mice at 5 weeks after DOX injection. (**b**) Graphic representation of relative protein level of p-Smad3 normalized against its total protein. The mRNA level of the target genes of Wnt/β-catenin signaling (**c,d**) and the target genes of Notch signaling (**e**) in the renal cortex were determined by real-time polymerase chain reaction and presented as fold induction over control. Data are expressed as mean ± SD, $N = 5$. *$P < 0.05$ versus control (CTRL) group. #$P < 0.05$ versus the adriamycin (ADR) group. GAPDH, glyceraldehyde-3-phosphate dehydrogenase. To optimize viewing of this image, please see the online version of this article at www.kidney-international.org.

such as *CCL2*, *CCL20*, *ICAM-1*, and *Fas* were decreased in P-NICLO–treated mice (Supplementary Figure S3D and E). Collectively, these data suggest that P-NICLO attenuates established renal interstitial fibrosis by inhibiting HIPK2 expression and the activation of its downstream profibrotic and proinflammatory pathways.

## DISCUSSION

In the current study, we demonstrated for the first time that P-NICLO exerts an antifibrotic effect on renal fibrosis in mouse models. ADR-induced kidney damage is characterized by initial podocyte injury, proteinuria, and late-onset renal fibrosis.[25,26] Administration of P-NICLO significantly attenuated glomerulosclerosis and interstitial fibrosis induced by ADR, suggesting a potent antifibrotic effect of P-NICLO. Moreover, later administration of P-NICLO (7 days after UUO) is capable of ameliorating established renal fibrosis. To the best of our knowledge, this is the first study showing that P-NICLO has a potent antifibrotic effect on preventing the progression of renal fibrosis but also mitigating established renal fibrosis.

Proteinuria is an early pathologic feature of many primary glomerular diseases but also an important pathogenic mediator that triggers subsequent inflammatory and fibrotic responses in renal parenchyma.[27] The effect of P-NICLO on ameliorating proteinuria induced by ADR suggests that P-NICLO might exert a protective effect on podocyte dysfunction and glomerular lesions. In support, we demonstrated that P-NICLO is capable of inhibiting Notch signaling, a pathway involved in podocyte injury.[28,29]

Another major finding of this study is that P-NICLO attenuates renal fibrosis by inhibiting TGF-β–induced HIPK2 expression. This conclusion is supported by the following data: (i) Western blot and real-time PCR revealed that P-NICLO directly inhibited TGF-β–induced HIPK2 transcription in a dose-dependent manner; (ii) P-NICLO inhibited HIPK2 expression in both ADR and UUO models; and (iii) P-NICLO blocked the activation of Smad, Notch, Wnt/β-catenin, and NF-κB signaling, which are downstream pathways of HIPK2. Overexpression of HIPK2 partially diminished the inhibitory effect of P-NICLO, suggesting that P-NICLO affects renal fibrosis through both HIPK2-dependent and -independent pathways. In this study, we found that P-NICLO decreased the mRNA level of HIPK2. Chromatin immunoprecipitation assay demonstrated that P-NICLO directly inhibits the binding of Smad3 on the promoter region of human HIPK2 genes, indicating that P-NICLO directly modulates HIPK2 transcription. Because

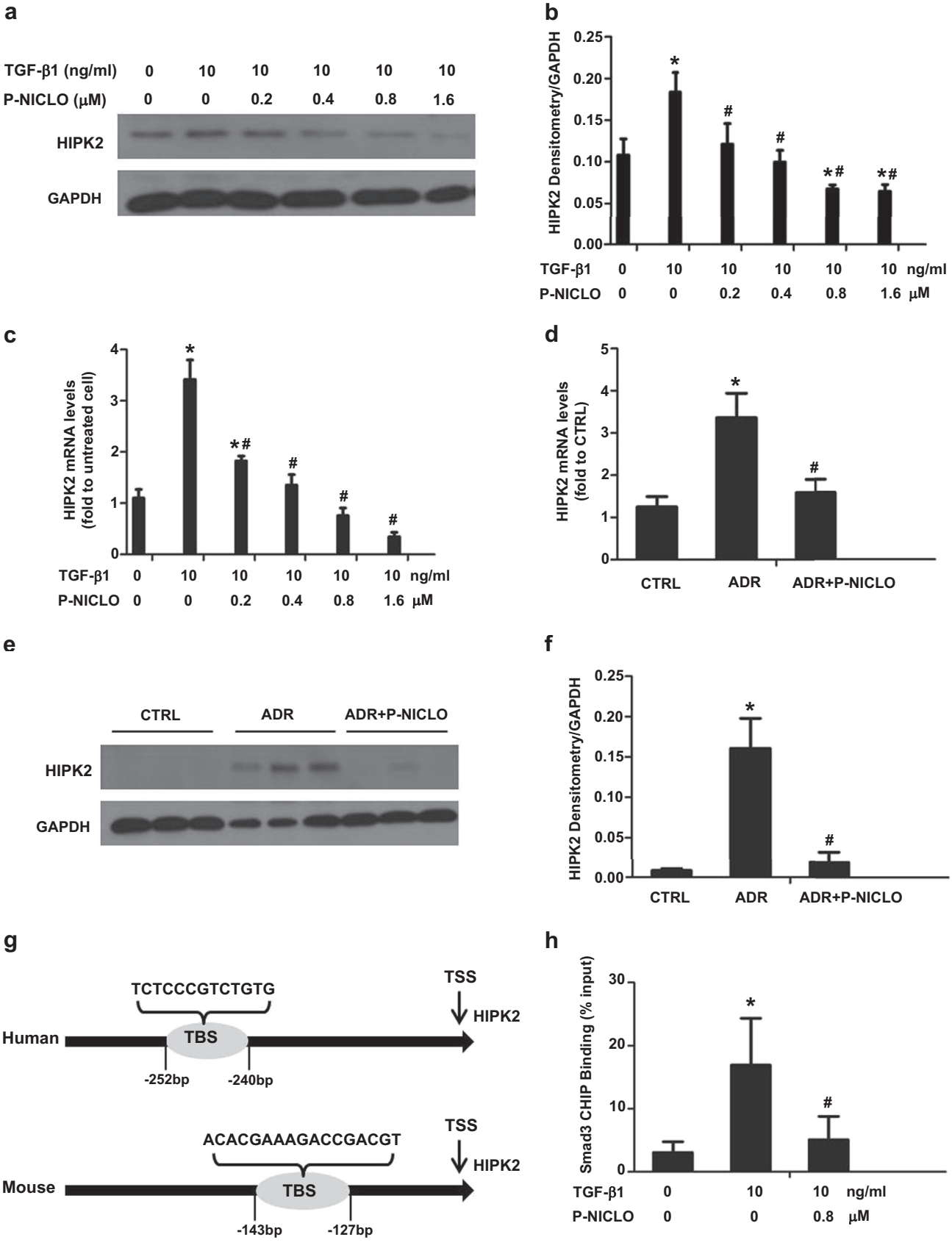
a
TGF-β1 (ng/ml) 0 10 10 10 10 10
P-NICLO (μM) 0 0 0.2 0.4 0.8 1.6
HIPK2
GAPDH
b
HIPK2 Densitometry/GAPDH
0.25
0.20
0.15
0.10
0.05
0.00
TGF-β1 0 10 10 10 10 10 ng/ml
P-NICLO 0 0 0.2 0.4 0.8 1.6 μM
c
HIPK2 mRNA levels (fold to untreated cell)
TGF-β1 0 10 10 10 10 10 ng/ml
P-NICLO 0 0 0.2 0.4 0.8 1.6 μM
d
HIPK2 mRNA levels (fold to CTRL)
CTRL
ADR
ADR+P-NICLO
e
CTRL
ADR
ADR+P-NICLO
HIPK2
GAPDH
f
HIPK2 Densitometry/GAPDH
CTRL
ADR
ADR+P-NICLO
g
TCTCCCGTCTGTG
TSS
HIPK2
Human
TBS
-252bp
-240bp
ACACGAAAGACCGACGT
TSS
HIPK2
Mouse
TBS
-143bp
-127bp
h
Smad3 CHIP Binding (% input)
TGF-β1 0 10 10 ng/ml
P-NICLO 0 0 0.8 μM

HIPK2 activates Smad3, our finding suggests that HIPK2 and TGF-β/Smad3 are regulated by each other to form a vicious cycle. HIPK2 has also been identified as a key regulator in idiopathic pulmonary fibrosis.[10,11] It will be interesting to test the antifibrotic effect of P-NICLO on idiopathic pulmonary fibrosis.

Renal fibrosis is a multifactorial chronic disease characterized by the activation of several profibrotic pathways.[4,30] Therefore, instead of targeting a single molecule or single pathway, drugs that are aimed at different components of the fibrotic process may be more likely to be effective. HIPK2 acts upstream of several major fibrosis signaling pathways and therefore might be a promising therapeutic target to reduce the progression of kidney fibrosis. However, some studies show that HIPK2 has oncosuppressor functions,[31,32] which makes people worry about the potential side effect of HIPK2 inhibitors on tumor growth; whereas P-NICLO has been shown to exert antitumor activity.[13,14,18,20] Therefore, P-NICLO might be a promising antifibrotic therapy without the potential side effect of oncogenesis.

In summary, we have shown that P-NICLO is effective in slowing the progression of renal fibrosis. Mechanistically, P-NICLO directly attenuated the activation of multiple proinflammatory and profibrotic signals through suppressing TGF-β1–induced HIPK2 expression. In addition, we did not observe obvious body weight loss or morphologic changes in liver or kidney tissues after continuous administration of P-NICLO (30 mg/kg per day) by i.p. injection for 3 weeks. Moreover, our preliminary data show that P-NICLO could be administered orally, although the bioavailability is lower than that of i.v. injection (data not shown). These data suggest that P-NICLO might be a potential therapeutic agent for renal fibrosis and is worthy of further investigation.

## MATERIALS AND METHODS

### Materials

P-NICLO was prepared as described previously.[13] ADR (doxorubicin HCl) was purchased from Sigma-Aldrich (St. Louis, MO). The primary antibodies used in this study are as follows: anti-p-Smad3 (#9520), anti-Smad3 (#9523) anti-p-p65 (#3033) were purchased from Cell Signaling Technology (Beverly, MA). Anti–α-SMA (A5228), anti-fibronectin (F3648) were obtained from Sigma-Aldrich. Anti-collagen I (234167) was purchased from Calbiochem (EMD Biosciences, Darmstadt, Germany). Anti-F4/80(14-4801) was obtained from eBioscience (Thermo Fisher, Grand Island, NY). Anti-CD3 (sc20047), anti-p65 (sc372), and anti-HIPK2 (sc10294) were obtained from Santa Cruz Biotechnology (Santa Cruz, CA).

### Animal experiments

Male BALB/C mice weighing 20 to 25 g were randomly divided into 3 groups: (i) control (CTRL) group ($N = 5$); (ii) ADR group ($N = 5$), and (iii) ADR+ P-NICLO group ($N = 5$). ADR (12 mg/kg) was injected once via the tail vein, as described previously.[25,26] CTRL mice were injected with same volume of isotonic saline. ADR+ P-NICLO group received an i.p. injection of P-NICLO (30 mg/kg per day) 2 weeks after ADR injection. All mice were killed 5 weeks after ADR injection.

UUO was performed using an established protocol, as described previously.[33] Briefly, the left ureter was ligated twice using 4-0 nylon surgical sutures at the level of the lower pole of the kidney. Male BALB/C mice weighing 20 to 25 g were randomly divided into 3 groups: (i) sham-operated group ($N = 5$); (ii) UUO group ($N = 5$), and (iii) UUO + P-NICLO group ($N = 5$). The mice in the UUO + P-NICLO group received an i.p. injection of P-NICLO (30 mg/kg per day) 7 days after the operation. All mice were killed at day 14 post-surgery. All mice work was performed in accordance with the protocol approved by the Ethics Committee for Animal Experiments of the Southern Medical University.

### Cell culture and treatment

Normal rat kidney epithelial cells (NRK52E) were cultured in DMEM/F12 medium supplemented with 10% fetal bovine serum (Gibco/Life Technologies, Grand Island, NY). When ~60% confluence was reached, cells were switched to serum-free medium overnight and then preincubated with the indicated amount of P-NICLO for 1 hour followed by coincubation with recombinant TGF-β1 (R&D Systems, Minneapolis, MN) for 24 hours.

### HIPK2 transfection

WT-HIPK2 construct was obtained from Dr. John Cijiang He, Mount Sinai School of Medicine, New York, NY. HK-2 cells were cultured in Dulbecco's modified Eagle/F12 medium supplemented with 10% fetal bovine serum. WT-HIPK2 construct was transfected into HK-2 cells by using Lipofectamin 2000 Reagent (cat. no. 1793393, Invitrogen, Carlsbad, CA) 24 hours after TGF-β1 (10 ng/ml) and P-NICLO (0.4 μM) treatment.

**Figure 4 | Phosphate of niclosamide (P-NICLO) inhibits homeodomain-interacting protein kinase 2 (HIPK2) expression by inhibiting the binding of Smad3 to the promoter of the *HIPK2* gene.** (**a–c**) P-NICLO inhibits transforming growth factor-β1 (TGF-β1)–induced HIPK2 expression *in vitro*. NRK52E cells were preincubated with or without indicated doses of P-NICLO for 1 hour and then stimulated with TGF-β1 (10 ng/ml) for 24 hours. (**a**) Protein level of HIPK2 was analyzed by Western blotting. (**b**) Graphic representation of relative protein level of HIPK2 normalized with glyceraldehyde-3-phosphate dehydrogenase (GAPDH). (**c**) Quantitative real-time polymerase chain reaction (PCR) shows the mRNA level of HIPK2. Data are expressed as mean ± SD of 3 independent experiments. *$P < 0.05$ versus untreated cells. #$P < 0.05$ versus TGF-β1–treated cells. (**d–f**) P-NICLO inhibits HIPK2 expression in ADR nephropathy. Quantitative real-time PCR and Western blots show the mRNA (**d**) and protein (**e**) levels of HIPK2 in different groups of mice at 5 weeks after DOX injection. (**f**) Graphic representation of relative intensities of HIPK2 normalized with GAPDH. Data are expressed as mean ± SD, $N = 5$. *$P < 0.05$ versus control (CTRL) group. #$P < 0.05$ versus DOX group. (**g**) Schematic graphs show the putative transfactor binding site (TBS) of Smad3 on the promoter of the human and murine *HIPK2* gene. The sequence and position of the putative Smad3 TBS in HIPK2 gene were marked. TSS, transcription start site. (**h**) HK-2 cells were preincubated with or without 0.8 μM of P-NICLO for 1 hour and then stimulated with TGF-β1 (10 ng/ml) for 24 hours. Cell lysates were harvested for chromatin immunoprecipitation (ChIP) assay by using anti-Smad3 antibody. The changes in Smad3 on the promoter of the *HIPK2* gene were examined by quantitative ChIP PCR. Data are expressed as the mean ± SD of 4 independent experiments. *$P < 0.05$ versus untreated cells. #$P < 0.05$ versus TGF-β1–treated cells. To optimize viewing of this image, please see the online version of this article at www.kidney-international.org.

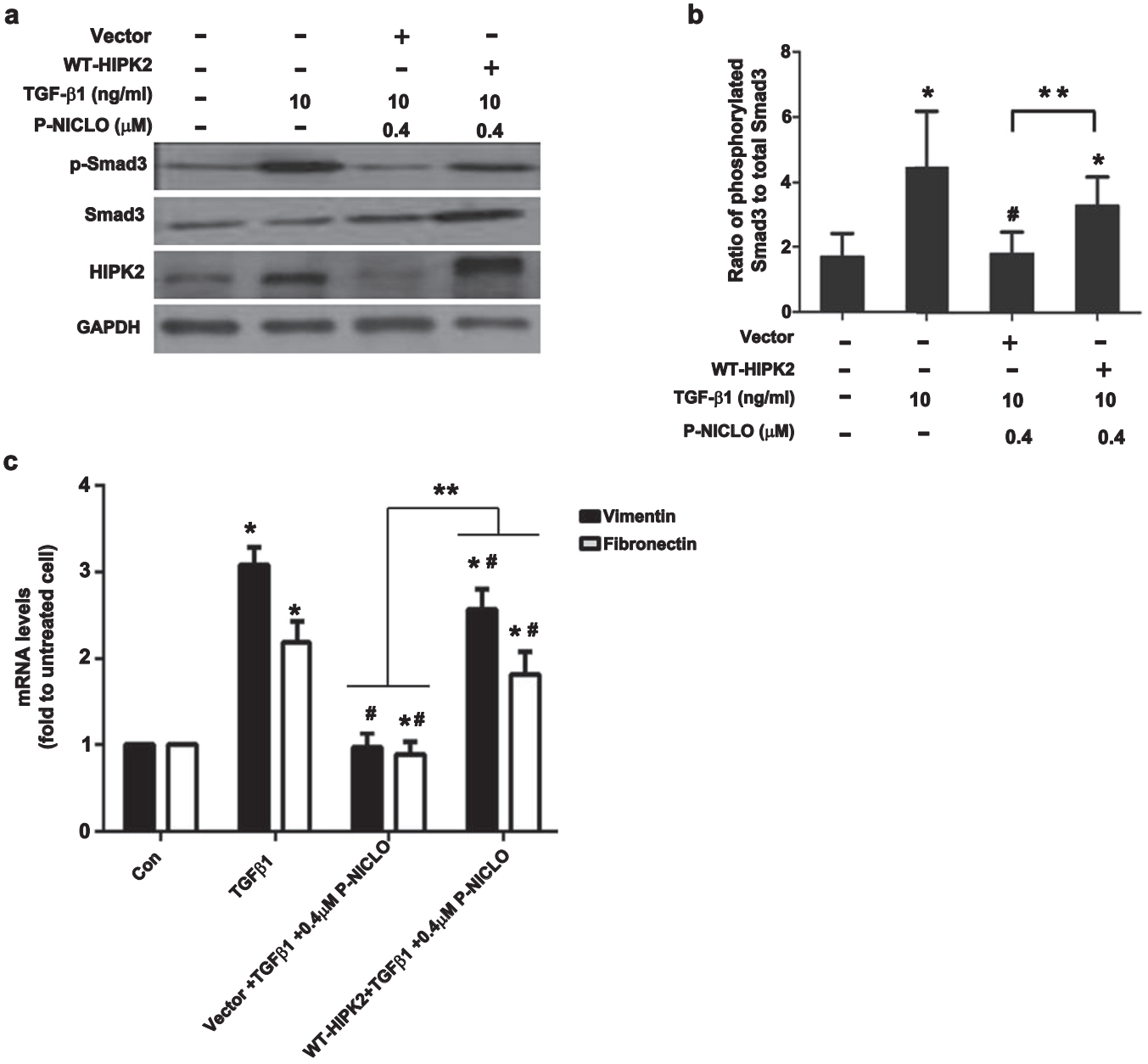


**Figure 5 | Overexpression of homeodomain-interacting protein kinase 2 (HIPK2) partially diminished the inhibitory effect of phosphate of niclosamide (P-NICLO).** HK-2 cells transfected with a wild-type HIPK2 construct (WT-HIPK2) or empty vector were incubated with transforming growth factor-β1 (TGF-β1) (10 ng/ml) in the presence or absence of P-NICLO (0.4 μM). (**a**) Representative Western blots show the protein level of HIPK2 and p-Smad3. (**b**) Graphic representation of relative protein level of p-Smad3 normalized against its total protein. (**c**) Quantitative real-time polymerase chain reaction was performed to analyze the mRNA level of vimentin and fibronectin. Data are expressed as the mean ± SD of 3 independent experiments. *$P < 0.05$ versus untreated cells. #$P < 0.05$ versus TGF-β–treated cells. **$P < 0.05$ versus TGF-β1– and P-NICLO–treated cells. Con, control group; GAPDH, glyceraldehyde-3-phosphate dehydrogenase. To optimize viewing of this image, please see the online version of this article at www.kidney-international.org.

### Chromatin immunoprecipitation assay

Chromatin immunoprecipitation assay was performed as described previously.[34,35] Briefly, HK-2 cells were preincubated with or without 0.8 μM of P-NICLO for 1 hour and then stimulated with TGF-β1 (10 ng/ml) for 24 hours. The cells were cross-linked with 1% formaldehyde for 10 minutes at room temperature and then lysed to obtain nuclear extract and digested to obtain chromatin segments (200–1000 bp) using the chromatin immunoprecipitation assay kit (cat. no. 26156, Thermo Scientific, Waltham, MA) according to the manufacturer's instructions. The input controls were 10% nuclear extract. The anti-Smad3 (cat. no. 9523, CST Cell Signaling Technology, Beverly, MA) was added and incubated with nuclear extract at 4 °C overnight, and IgG was a negative control. Protein A/G was added to collect the immune complex and incubate with shaking for 1 hour at 4 °C. DNA was purified and recovered for reverse transcriptase PCR per the kit instructions.

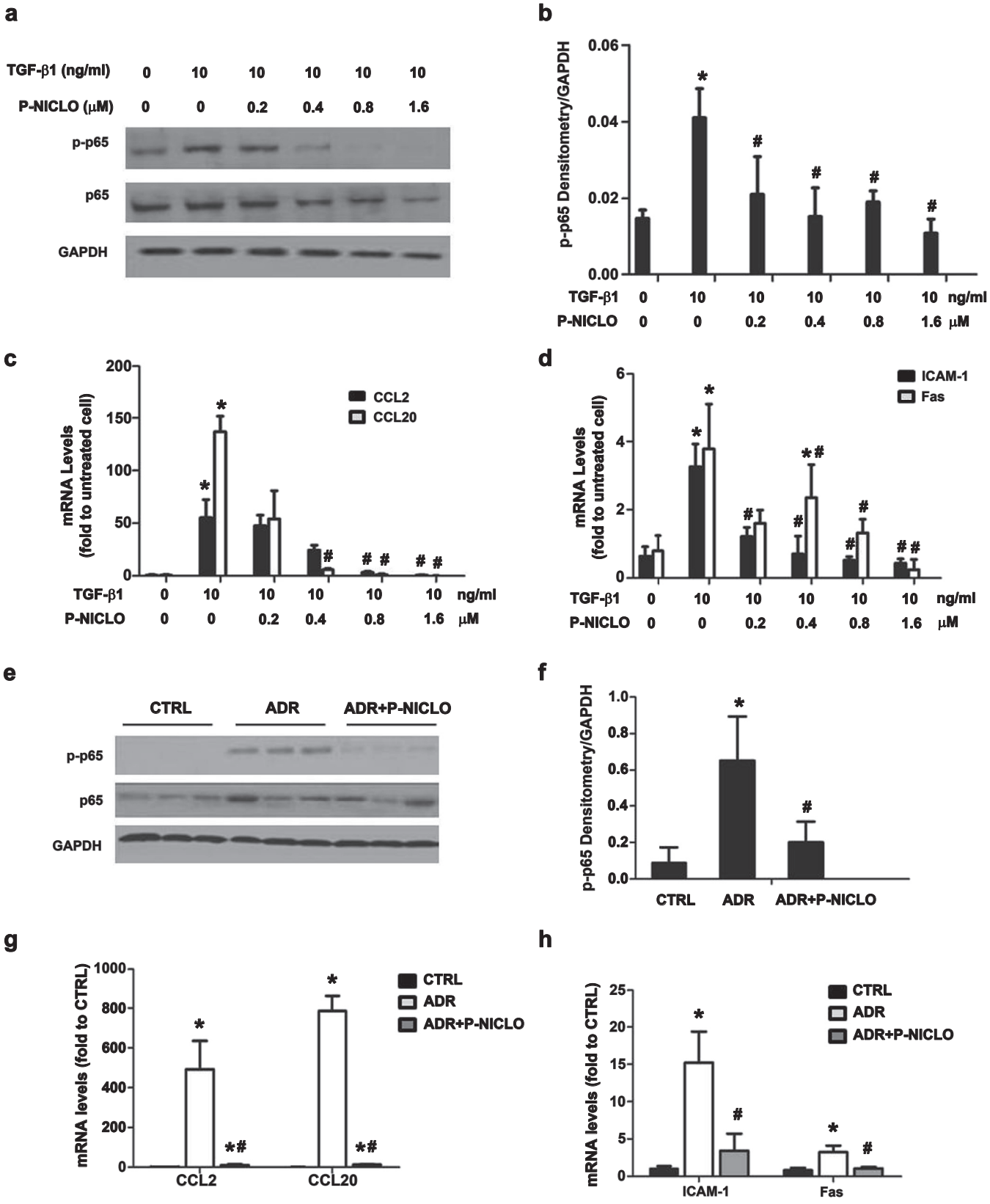


**Figure 6 | Phosphate of niclosamide (P-NICLO) ameliorates nuclear factor-κB (NF-κB) activation *in vitro* and *in vivo*.** (**a–d**) P-NICLO ameliorates NF-κB activation *in vitro*. NRK52E cells were preincubated with or without indicated doses of P-NICLO for 1 hour and then coincubated with transforming growth factor-β1 (TGF-β1) (10 ng/ml) for 24 hours. (**a**) The protein level of p-p65 and p65 were analyzed by Western blot. (**b**) Graphic representation of relative protein level of p-p65 normalized with glyceraldehyde-3-phosphate dehydrogenase (GAPDH). (**c,d**) The mRNA levels of *CCL2*, *CCL20*, *ICAM-1*, and *Fas* were examined by real-time PCR and indicated as fold induction over untreated cells. Data are (Continued)

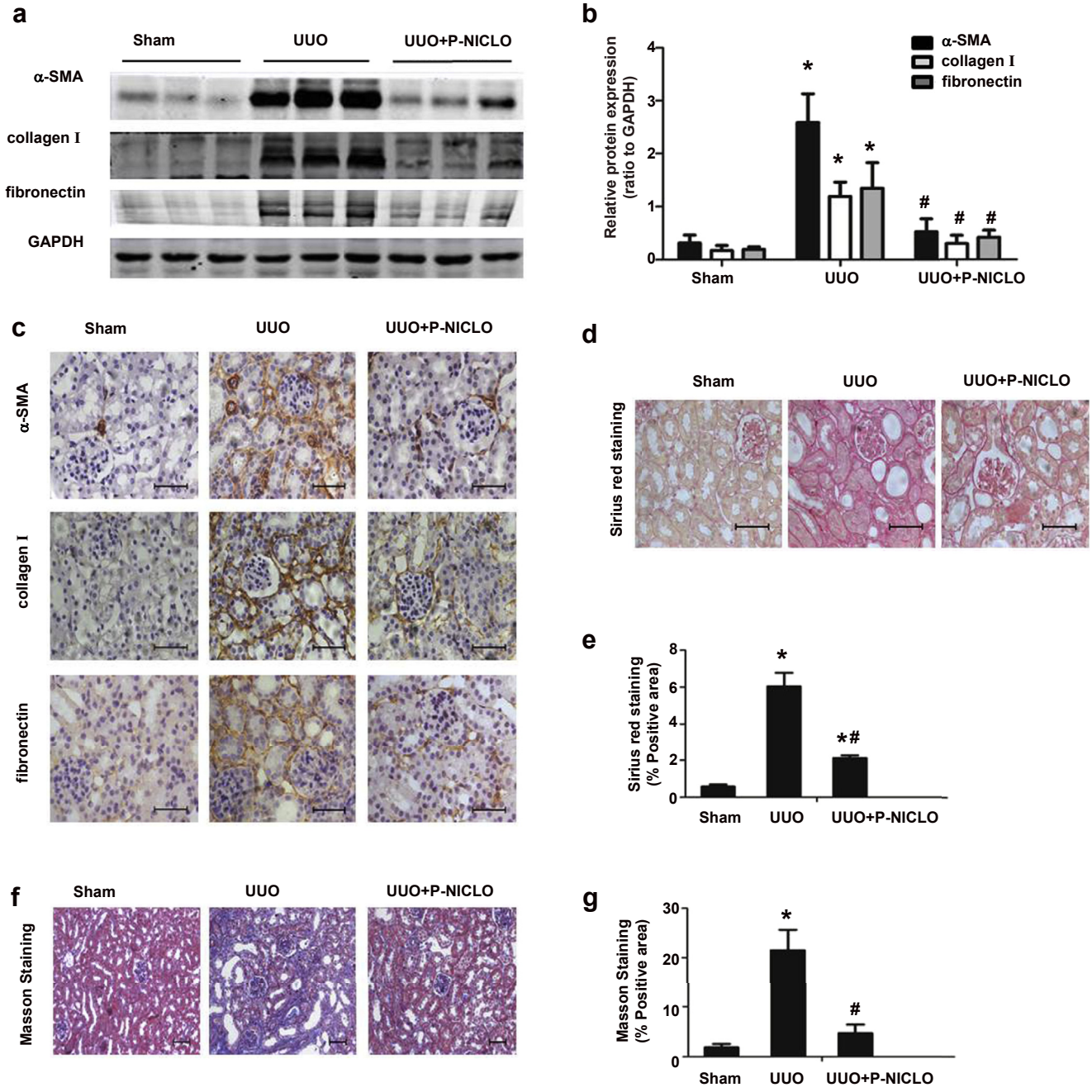


**Figure 7 | Phosphate of niclosamide (P-NICLO) attenuates established interstitial fibrosis induced by unilateral ureteral obstruction (UUO).** Mice received daily i.p. injections of P-NICLO (30 mg/kg) at day 7 after UUO and were killed on day 14 after UUO. Representative Western blots (**a**) and quantitative determination (**b**) of the protein level of α-smooth muscle actin (α-SMA), collagen I, and fibronectin in the kidney cortex of different groups of mice are presented. (**c**) Representative micrographs of immunohistochemical staining of the expression and distribution of α-SMA, collagen I, and fibronectin in the renal cortex. Representative micrographs and quantitative assessment of collagen accumulation based on Sirius red (**d,e**) and Masson (**f,g**) staining are presented. Bar = 50 μm. Data are expressed as mean ± SD, $N = 5$. *$P < 0.05$ versus the Sham group. #$P < 0.05$ versus the UUO group. GAPDH, glyceraldehyde-3-phosphate dehydrogenase. To optimize viewing of this image, please see the online version of this article at www.kidney-international.org.

**Figure 6** | (Continued) expressed as the mean ± SD of 3 independent experiments. *$P < 0.05$ versus untreated cells. #$P < 0.05$ versus TGF-β1–treated cells. (**e–h**) P-NICLO ameliorates NF-κB activation in ADR nephropathy. (**e,f**) Representative Western blot and quantitative assessment of the protein level of p-p65 in the renal cortex of different groups of mice at 5 weeks after DOX injection. (**g,h**) The mRNA levels of *CCL2*, *CCL20*, *ICAM-1*, and *Fas* in the renal cortex tissues were examined by real-time polymerase chain reaction and indicated as fold induction over control mice. Data are expressed as mean ± SD, $N = 5$. *$P < 0.05$ versus the control (CTRL) group. #$P < 0.05$ versus the adriamycin (ADR) group. To optimize viewing of this image, please see the online version of this article at www.kidney-international.org.

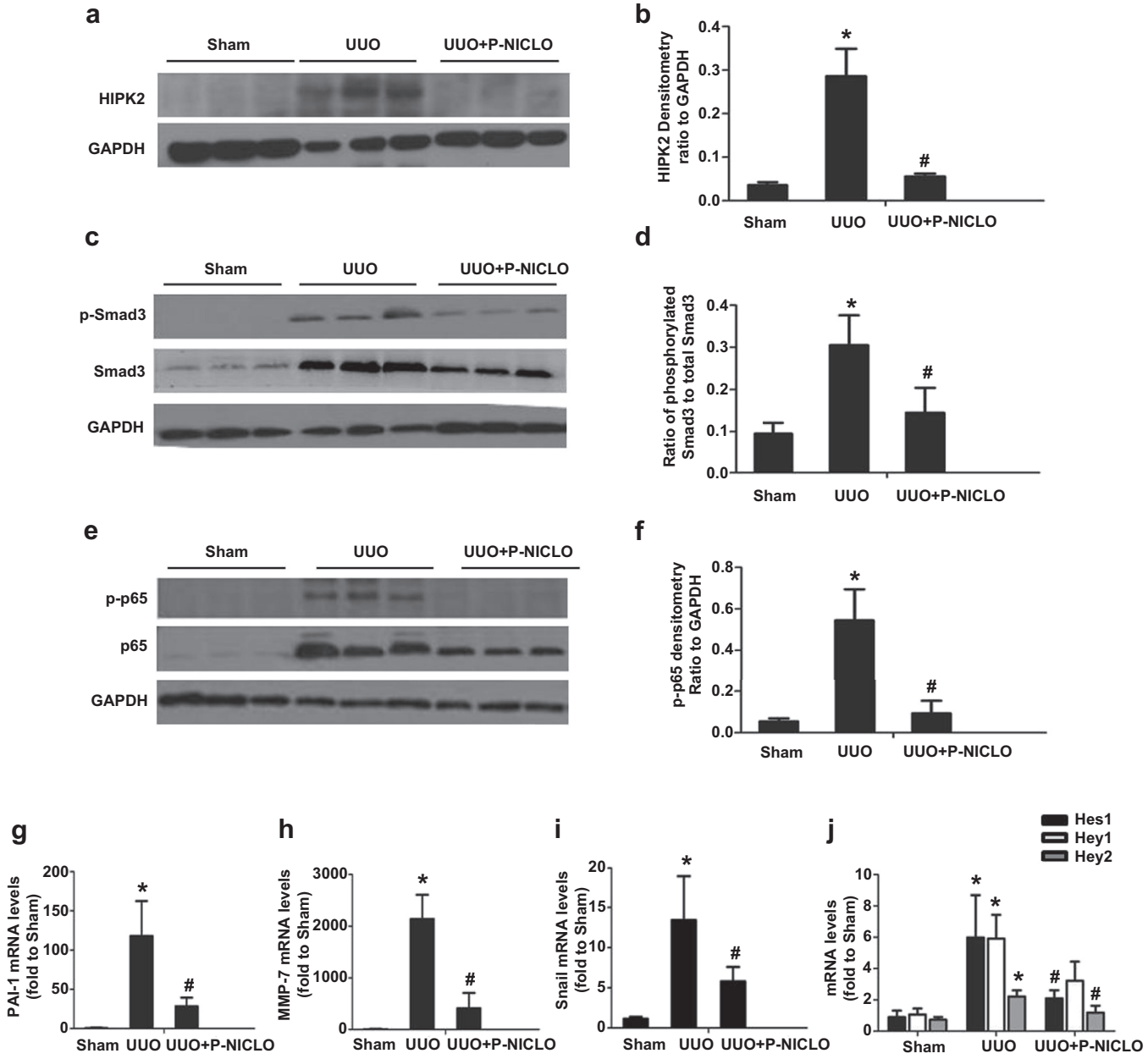


**Figure 8 | Phosphate of niclosamide (P-NICLO) inhibits homeodomain-interacting protein kinase 2 (HIPK2) expression and its downstream signaling pathways in unilateral ureteral obstruction (UUO).** Mice received daily i.p. injections of P-NICLO (30 mg/kg) at day 7 after UUO and were killed on day 14 after UUO. Representative Western blots (**a,c,e**) and quantitative determination (**b,d,f**) of the protein level of HIPK2, p-Smad3, and p-p65 in renal cortex of different groups of mice at 14 days after UUO. (**g–j**) The mRNA level of the target genes of Wnt/β-catenin and Notch signaling in the renal cortex of different groups of mice at 14 days after UUO are presented. Data are expressed as mean ± SD, $N = 5$. *$P < 0.05$ versus the Sham group. #$P < 0.05$ versus the UUO group. To optimize viewing of this image, please see the online version of this article at www.kidney-international.org.

The sequences of primers used in this study were as follows: human HIPK2, forward 5′-CCGGCCCTCTCACCCAC-3′; reverse 5′-GATGCGAGGCGGGGAAG-3′.

### Urine albumin and creatinine assay

Urine albumin was measured by using a mouse albumin enzyme-linked immunosorbent assay quantitation kit according to the manufacturer's protocol (Bethyl Laboratories, Inc., Montgomery, TX). Urine creatinine was determined by a routine procedure according to the manufacturer's protocol (Bioassay Systems, Hayward, CA). Urinary proteins were normalized against urinary creatinine.

### MTT assay

NRK52E cells were seeded into 96-well plates in a volume of 200 μl per well ($1 \times 10^5$ cells/ml) and incubated for 24 hours to allow cells to attach. The cells were then incubated with the indicated amount of P-NICLO for 24 hours. Cell viability was determined by addition of 20 μl of MTT(3-[4,5-dimethylthiazol-2-yl]-2,5-

diphenyltetrazolium bromide) at a concentration of 5 mg/ml. After incubation for 4 hours, the medium was removed, and 150 μl of DMSO was added to dissolve the formazan crystals. The absorbance was read at 490 nm by using an iMark Microplate Reader (Multiskan GO, Thermo Scientific).

### Histology

Paraffin-embedded kidney sections (2 μm) were stained with periodic acid–Schiff, Masson trichrome, and Sirius red. These stainings are according to the manufacturer's protocol. The glomerulosclerosis index was scored on a scale of 0 to 4 based on the percentage of glomerulus area of periodic acid–Schiff staining positive (0, <5%; 1, 5%–25%; 2, 25%–50%; 3, 50%–75%; and 4, >75%. Sirius red and Masson-trichrome staining were evaluated by calculating the average area of staining positive (%). At least 10 randomly chosen fields in the cortex under the microscope (×400), Masson-trichrome staining (×200) were evaluated for each mouse in a blinded manner.

### Immunohistochemical staining

Immunohistochemical staining was performed on 4-μm kidney sections as previously described.[36] After antigen retrieval, sections were incubated with the primary antibody against α-SMA, collagen I, fibronectin, CD3, and F4/80, respectively, and then detected by the En Vision/HRP Kit (Dako, Carpinteria, CA).

### Western blot

Cells or kidney tissues were lysed with protein cracking liquid lysis buffer (25 mM Tris-HCl, 150 mM NaCl, 1% Nonidet P-40, and 10 mM ethylenediamine tetraacetic acid, pH 8.0, 1% protease inhibitor cocktail) for 30 minutes on ice. Lysates were subjected to Western blot analysis using the method described previously.[37,38] The following primary antibodies were used: anti-HIPK2, anti–α-SMA, antifibronectin, anti-collagen I, anti–p-Smad3, anti-Smad3, anti–p-p65, and anti-p65.

### Real-time PCR

Total RNA was isolated from cells (NRK52E, HK-2) or kidney tissues using TRIzol reagent according to the manufacturer's instructions (Invitrogen). Real-time PCR was performed on an ABI PRISM 7500 Fast sequence detection system (Applied Biosystems, Foster City, CA). The mRNA levels of various genes were calculated after normalizing with glyceraldehyde-3-phosphate dehydrogenase by the comparative CT method ($2^{-\Delta\Delta Ct}$). The primers used in the experiments are listed in Supplementary Tables S1–3.

### Statistical analysis

Data are expressed as the mean ± SD. Comparisons between 2 groups were analyzed using the 2-tailed $t$ test. Comparisons between groups were made using 1-way analysis of variance followed by the Student-Newman-Keuls test (IBM SPSS software, version 19.0). $P < 0.05$ was considered statistically significant.

### DISCLOSURE

All the authors declared no competing interests.

### ACKNOWLEDGMENTS

This work was supported by grants from the Nature and Science Foundation of China (81288001, 81521003) and the Natural Science Foundation of Guangdong Province (S2013020012748) to Dr. Jing Nie.

### SUPPLEMENTARY MATERIAL

**Figure S1.** MTT assay. NRK52E cells were treated with indicated amount of phosphate of niclosamide (P-NICLO) for 24 hours and then washed for the MTT assay. Data are expressed as mean ± SD of 3 independent experiments.

**Figure S2.** Phosphate of niclosamide (P-NICLO) inhibits proinflammatory cytokine production in ADR nephropathy. The mRNA levels of monocyte chemotactic protein-1 (MCP-1), tumor necrosis factor-α (TNF-α), and interleukin-6 (IL-6) in renal cortex of different groups of mice at 5 weeks after ADR injection were examined by real-time polymerase chain reaction and indicated as fold induction over control mice. Data are expressed as mean ± SD, $N = 5$. *$P < 0.05$ versus control (CTRL) group. #$P < 0.05$ versus ADR group.

**Figure S3.** Phosphate of niclosamide (P-NICLO) attenuates interstitial inflammation in unilateral ureteral obstruction (UUO). Representative micrographs of immunohistochemical staining (**A**) and quantitative assessment (**B,C**) of F4/80-positive and CD3-positive cells in different groups of mice at 14 days after UUO. (**D,E**) The renal mRNA levels of nuclear factor-κB target genes *CCL2*, *CCL20*, *ICAM-1*, and *Fas* at 14 days after UUO were determined by quantitative real-time polymerase chain reaction and indicated as fold induction over control. Bar = 50 μm. Data are expressed as mean ± SD, $N = 5$. *$P < 0.05$ versus Sham group. #$P < 0.05$ versus UUO group.

**Table S1.** List of mice primers used for quantitative reverse-transcriptase polymerase chain reaction.

**Table S2.** List of rat primers used for quantitative reverse-transcriptase polymerase chain reaction.

**Table S3.** List of human primers used for quantitative reverse-transcriptase polymerase chain reaction.

Supplementary material is linked to the online version of the paper at www.kidney-international.org.

### REFERENCES

1. Levey AS, Atkins R, Coresh J, et al. Chronic kidney disease as a global public health problem: approaches and initiatives - a position statement from Kidney Disease Improving Global Outcomes. *Kidney Int*. 2007;72:247–259.
2. Hill NR, Fatoba ST, Oke JL, et al. Global prevalence of chronic kidney disease - a systematic review and meta-analysis. *PLoS One*. 2016;11:e158765.
3. Liu Y. Cellular and molecular mechanisms of renal fibrosis. *Nat Rev Nephrol*. 2011;7:684–696.
4. Zeisberg M, Neilson EG. Mechanisms of tubulointerstitial fibrosis. *J Am Soc Nephrol*. 2010;21:1819–1834.
5. Chuang PY, Menon MC, He JC. Molecular targets for treatment of kidney fibrosis. *J Mol Med (Berl)*. 2013;91:549–559.
6. Duffield JS, Lupher M, Thannickal VJ, Wynn TA. Host responses in tissue repair and fibrosis. *Annu Rev Pathol*. 2013;8:241–276.
7. Hou FF, Liu Y. New insights into the pathogenesis and therapeutics of kidney fibrosis. *Kidney Int Suppl (2011)*. 2014;4:1.
8. Jin Y, Ratnam K, Chuang PY, et al. A systems approach identifies HIPK2 as a key regulator of kidney fibrosis. *Nat Med*. 2012;18:580–588.
9. Fan Y, Wang N, Chuang P, He JC. Role of HIPK2 in kidney fibrosis. *Kidney Int Suppl (2011)*. 2014;4:97–101.
10. Saul VV, Schmitz ML. Posttranslational modifications regulate HIPK2, a driver of proliferative diseases. *J Mol Med (Berl)*. 2013;91:1051–1058.
11. Ricci A, Cherubini E, Ulivieri A, et al. Homeodomain-interacting protein kinase2 in human idiopathic pulmonary fibrosis. *J Cell Physiol*. 2013;228:235–241.
12. Nugent MM, Lee K, He JC. HIPK2 is a new drug target for anti-fibrosis therapy in kidney disease. *Front Physiol*. 2015;6:132.
13. Pan JX, Ding K, Wang CY. Niclosamide, an old antihelminthic agent, demonstrates antitumor activity by blocking multiple signaling pathways of cancer stem cells. *Chin J Cancer*. 2012;31:178–184.
14. Li Y, Li PK, Roberts MJ, et al. Multi-targeted therapy of cancer by niclosamide: a new application for an old drug. *Cancer Lett*. 2014;349:8–14.
15. Weinbach EC, Garbus J. Mechanism of action of reagents that uncouple oxidative phosphorylation. *Nature*. 1969;221:1016–1018.
16. Balgi AD, Fonseca BD, Donohue E, et al. Screen for chemical modulators of autophagy reveals novel therapeutic inhibitors of mTORC1 signaling. *PLoS One*. 2009;4:e7124.
17. Khanim FL, Merrick BA, Giles HV, et al. Redeployment-based drug screening identifies the anti-helminthic niclosamide as anti-myeloma

therapy that also reduces free light chain production. *Blood Cancer J*. 2011;1:e39.
18. Wang YC, Chao TK, Chang CC, et al. Drug screening identifies niclosamide as an inhibitor of breast cancer stem-like cells. *PLoS One*. 2013;8:e74538.
19. Mercer-Haines N, Fioravanti CF. Hymenolepis diminuta: mitochondrial transhydrogenase as an additional site for anaerobic phosphorylation. *Exp Parasitol*. 2008;119:24–29.
20. Jin Y, Lu Z, Ding K, et al. Antineoplastic mechanisms of niclosamide in acute myelogenous leukemia stem cells: inactivation of the NF-kappaB pathway and generation of reactive oxygen species. *Cancer Res*. 2010;70:2516–2527.
21. Chen M, Wang J, Lu J, et al. The anti-helminthic niclosamide inhibits Wnt/Frizzled1 signaling. *Biochemistry*. 2009;48:10267–10274.
22. Osada T, Chen M, Yang XY, et al. Antihelminth compound niclosamide downregulates Wnt signaling and elicits antitumor responses in tumors with activating APC mutations. *Cancer Res*. 2011;71:4172–4182.
23. Wang AM, Ku HH, Liang YC, et al. The autonomous notch signal pathway is activated by baicalin and baicalein but is suppressed by niclosamide in K562 cells. *J Cell Biochem*. 2009;106:682–692.
24. Wieland A, Trageser D, Gogolok S, et al. Anticancer effects of niclosamide in human glioblastoma. *Clin Cancer Res*. 2013;19:4124–4136.
25. Wang Y, Wang YP, Tay YC, Harris DC. Progressive adriamycin nephropathy in mice: sequence of histologic and immunohistochemical events. *Kidney Int*. 2000;58:1797–1804.
26. Wang YM, Wang Y, Harris DC, et al. Adriamycin nephropathy in BALB/c mice. *Curr Protoc Immunol*. 2015;108:15–28.
27. Abbate M, Zoja C, Remuzzi G. How does proteinuria cause progressive renal damage? *J Am Soc Nephrol*. 2006;17:2974–2984.
28. Murea M, Park JK, Sharma S, et al. Expression of Notch pathway proteins correlates with albuminuria, glomerulosclerosis, and renal function. *Kidney Int*. 2010;78:514–522.
29. Sweetwyne MT, Tao J, Susztak K. Kick it up a notch: Notch signaling and kidney fibrosis. *Kidney Int Suppl (2011)*. 2014;4:91–96.
30. Schlondorff DO. Overview of factors contributing to the pathophysiology of progressive renal disease. *Kidney Int*. 2008;74:860–866.
31. Nardinocchi L, Puca R, Givol D, D'Orazi G. HIPK2-a therapeutical target to be (re)activated for tumor suppression: role in p53 activation and HIF-1alpha inhibition. *Cell Cycle*. 2010;9:1270–1275.
32. de la Vega L, Grishina I, Moreno R, et al. A redox-regulated SUMO/acetylation switch of HIPK2 controls the survival threshold to oxidative stress. *Mol Cell*. 2012;46:472–483.
33. Klahr S, Morrissey J. Obstructive nephropathy and renal fibrosis. *Am J Physiol Renal Physiol*. 2002;283:F861–F875.
34. Das PM, Ramachandran K, VanWert J, Singal R. Chromatin immunoprecipitation assay. *Biotechniques*. 2004;37:961–969.
35. Pan XY, Zhao W, Zeng XY, et al. Heat shock factor 1 mediates latent HIV reactivation. *Sci Rep*. 2016;6:26294.
36. Remuzzi G, Zoja C, Gagliardini E, et al. Combining an antiproteinuric approach with mycophenolate mofetil fully suppresses progressive nephropathy of experimental animals. *J Am Soc Nephrol*. 1999;10:1542–1549.
37. Chiang CK, Sheu ML, Hung KY, et al., a small molecular weight natural product, alleviates experimental mesangial proliferative glomerulonephritis. *Kidney Int*. 2006;70:682–689.
38. Sheu ML, Liu SH, Lan KH. Honokiol induces calpain-mediated glucose-regulated protein-94 cleavage and apoptosis in human gastric cancer cells and reduces tumor growth. *PLoS One*. 2007;2:e1096.